

Normal Multi-Scale Transforms for Surfaces

Peter Oswald

Jacobs University Bremen, School of Engineering and Science,
Campus Ring 1, 28759 Bremen, Germany
p.oswald@jacobs-university.de
<http://www.faculty.jacobs-university.de/poswald>

Abstract. We prove well-posedness, convergence, and detail decay estimates for the normal triangular mesh multi-scale transform for $C^{1,\alpha}$ surfaces in the simplest case when the subdivision rule S used for base point prediction is given by edge midpoint insertion. A restrictive assumption is that the initial triangular mesh needs to be quasi-regular and of small enough mesh-size. We also provide numerical evidence with other S for dyadic refinement (Butterfly, Loop), and propose a modification of the normal scheme resulting in improved detail decay for smooth surfaces.

Keywords: Nonlinear geometric multi-scale transforms, linear subdivision, surface representation, detail decay

1 Introduction

Normal multi-scale transforms (MTs) for curves and surfaces [7] are nonlinear MTs based on a linear subdivision operator S and a nonlinear transformation for the detail part involving approximate normal directions. They have been used for multi-scale representation and compression of geometric objects [12, 14, 4], for adaptive approximation of level curves [2], in image analysis [1], and recently for interface tracking [17]. Roughly speaking, normal MT starts from an initial triangular mesh on Σ (a curve in \mathbb{R}^2 or a surface in \mathbb{R}^3) represented by its vertex set \mathbf{v}^0 , and creates denser triangular meshes $\mathbf{v}^1, \mathbf{v}^2, \dots$ on Σ by recursively repeating the following steps:

- Given $\mathbf{v}^{j-1} \subset \Sigma$ and a linear subdivision scheme S for triangular meshes, a set $\hat{\mathbf{v}}^j = S\mathbf{v}^{j-1}$ of base points is computed, these points typically do not belong to Σ .
- Similarly, a set $\hat{\mathbf{n}}^j$ of approximate normals of unit length (one for each base point) is computed, e.g., by taking suitable averages of normal directions to the triangles in the mesh associated with \mathbf{v}^{j-1} .
- By finding the intersection points \mathbf{v}_i^j of the family of parametric "normal" lines $\hat{\mathbf{v}}_i^j + s\hat{\mathbf{n}}_i^j$ passing through the base points from $\hat{\mathbf{v}}^j$ in the direction given by the corresponding approximate normal from $\hat{\mathbf{n}}^j$ with Σ , one arrives at the new triangular mesh \mathbf{v}^j on Σ , and the sequence d^j of scalar details $d_i^j = (\mathbf{v}_i^j - \hat{\mathbf{v}}_i^j)\hat{\mathbf{n}}_i^j$ to be stored. This task is the most ambiguous one, as no

or many intersection points with Σ may exist resp. mesh obstructions may occur. The vector \mathbf{v}^j can be recovered from \mathbf{v}^{j-1} and d^j by first computing $\hat{\mathbf{v}}^j, \hat{\mathbf{n}}^j$ from \mathbf{v}^{j-1} , and then using the reconstruction formula

$$\mathbf{v}^j = \hat{\mathbf{v}}^j + d^j \hat{\mathbf{n}}^j,$$

where the multiplication $d^j \hat{\mathbf{n}}^j$ has to be executed entry-wise.

If, with proper specification of the intersection procedure and under certain conditions on \mathbf{v}^0 , this construction does not fail (well-posedness), we obtain the normal MT $\Sigma \rightarrow \{\mathbf{v}^0, d^1, d^2, \dots\}$ and can recover Σ as limit of triangular surfaces by computing $\mathbf{v}^j, j \geq 1$, using the reconstruction formula recursively.

Normal MTs for smooth curves in \mathbb{R}^2 have been investigated in [3, 16, 10], and are well-understood by now. In this note, we make a first step towards a theory of normal MTs for smooth surfaces in \mathbb{R}^3 by investigating the normal MT for $C^{1,\alpha}$ surfaces $\Sigma \subset \mathbb{R}^3$ with the simplest S (based on edge midpoint insertion) for triangular meshes. The definition and basic properties of this transform and the underlying triangular meshes will be introduced in Section 2. Our main result concerning the well-posedness, convergence, and guaranteed detail decay of order $O(2^{-j(1+\alpha)})$ of this MT for sufficiently dense and regular initial meshes will be stated and proved in Section 3. Section 4 discusses the possible extensions of this initial result to more general S , and provides numerical evidence on detail decay for smooth surfaces. In particular, we show that the influence of extraordinary vertices can practically be neglected. We also introduce a new normal multi-scale transform with improved detail decay, consisting of a clever combination of Loop subdivision (for predicting base points and approximate normals) and Butterfly subdivision (for predicting a point closer to the surface along the normal line).

2 Definitions and Preliminary Facts

2.1 Surfaces and Triangular Meshes

For the study of normal MTs for closed 2-dimensional $C^{1,\alpha}$ manifolds Σ embedded in \mathbb{R}^3 (the treatment of boundaries is beyond the scope of our investigation), due to the locality of the used subdivision rule and the density assumptions on the initial meshes \mathbf{v}^0 necessary for our asymptotic analysis, we may resort to graph surfaces $\Sigma = \{\mathbf{v}_P := (P, f(P)) : P := (x, y) \in \mathbb{R}^2\} \subset \mathbb{R}^3$ given by a $C^{1,\alpha}$ function $f : \mathbb{R}^2 \rightarrow \mathbb{R}$ with globally bounded gradient and Lipschitz constants, i.e., there are constants C_0, C_1 such that

$$|\mathbf{n}_P| = \sqrt{1 + |\nabla f(P)|^2} \leq C_0,$$

where $\mathbf{n}_P = (-\nabla f(P), 1)$ is the normal to the tangent plane to Σ at \mathbf{v}_P ,

$$|\nabla f(Q) - \nabla f(P)| \leq C_1 |Q - P|^\alpha, \quad P, Q \in \mathbb{R}^2,$$

and consequently also

$$f(Q) = f(P) + \nabla f(P)(Q - P) + R(P, Q), \quad |R(P, Q)| \leq C_1 |Q - P|^{1+\alpha},$$

where $P, Q \in \mathbb{R}^2$. Everywhere, $|\cdot|$ denotes the Euclidean norm in \mathbb{R}^d with $d = 1, 2, 3$, depending on context. Products of vectors in \mathbb{R}^d , if not specified otherwise, are to be understood as scalar products.

We consider triangular meshes on Σ generated by triangulations in \mathbb{R}^2 , i.e., if \mathcal{V} is the vertex set of a triangulation \mathcal{T} in \mathbb{R}^2 then $\mathbf{v} := \{\mathbf{v}_P : P \in \mathcal{V}\}$ represents the vertex set of a triangular mesh on Σ , with the mesh topology (edges, faces) inherited from \mathcal{T} . The global mesh-width $h(\mathbf{v})$ is defined as the supremum of all edge lengths $|\mathbf{e}|$, where $\mathbf{e} = \mathbf{e}_{PQ} = \mathbf{v}_Q - \mathbf{v}_P$ is the edge connecting neighboring vertices P and Q of \mathcal{T} . By $h_{\mathcal{T}}$ we denote the similarly defined mesh-width of \mathcal{T} . Since

$$|Q - P| \leq |\mathbf{e}| = |\mathbf{v}_Q - \mathbf{v}_P| \leq C_0 |Q - P| \quad (1)$$

we always have $h_{\mathcal{T}} \leq h(\mathbf{v}) \leq C_0 h_{\mathcal{T}}$. We call such a mesh given by \mathcal{T} and \mathbf{v} regular with regularity constant $c = \sin \gamma$, $\gamma \in (0, \pi/3]$ (or in short c -regular), if the interior angles of any triangular face of the mesh are $\geq \gamma$. More conveniently, this can be expressed by requiring the inequality

$$|\mathbf{e} \times \tilde{\mathbf{e}}| \geq c |\mathbf{e}| |\tilde{\mathbf{e}}|$$

to hold for any two edges of any triangular face of the mesh. Without detailed proof, we state the following elementary properties.

Proposition 1. *Let Σ be a $C^{1,\alpha}$ graph surface, and \mathbf{v} a c -regular triangular mesh on Σ , as described above.*

- a) *For any two edges \mathbf{e} and $\tilde{\mathbf{e}}$ belonging to the same face, we have $|\mathbf{e}|/|\tilde{\mathbf{e}}| \leq 1/c$.*
- b) *There is a $\bar{h}_1 > 0$ (depending on c, C_0 only) such that for $h(\mathbf{v}) \leq \bar{h}_1$, the underlying triangulation \mathcal{T} of \mathbb{R}^2 is \bar{c} -regular, with some other $\bar{c} \geq c/(2C_0)$. Conversely, if \mathcal{T} is \bar{c} -regular and $h_{\mathcal{T}}$ is small enough, then the associated triangular mesh on Σ is c -regular for some $c > \bar{c}/(2C_0^2)$.*

Since $|\mathbf{e} \times \tilde{\mathbf{e}}| = |\mathbf{e} \times \bar{\mathbf{e}}| = |\tilde{\mathbf{e}} \times \bar{\mathbf{e}}|$, where $\bar{\mathbf{e}}$ denotes the remaining edge of the triangular face under consideration, we have

$$\frac{|\mathbf{e}|}{|\tilde{\mathbf{e}}|} = \frac{|\mathbf{e}| |\bar{\mathbf{e}}|}{|\tilde{\mathbf{e}}| |\bar{\mathbf{e}}|} \leq \frac{c^{-1} |\mathbf{e} \times \bar{\mathbf{e}}|}{|\tilde{\mathbf{e}} \times \bar{\mathbf{e}}|} = \frac{1}{c}.$$

This gives part a). For part b), see the remarks in the proof of Proposition 2 below.

2.2 Approximate Normals

Normal MTs need a rule for creating approximate normals. In our case, base points are the midpoints of edges \mathbf{e} , and the property we need in the proofs is the existence of a constant C_2 such that

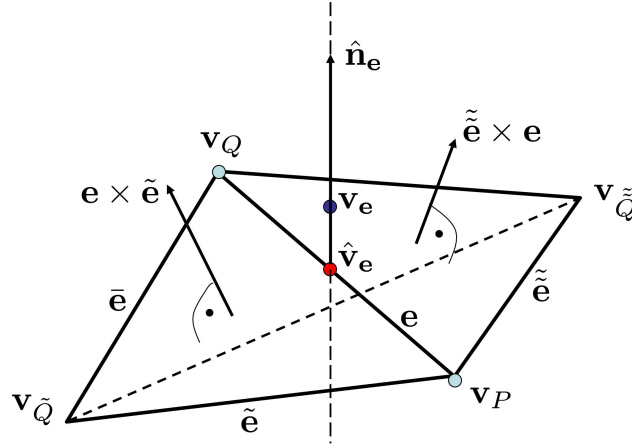
$$\min |\pm \hat{\mathbf{n}}_{\mathbf{e}} - \hat{\mathbf{n}}_P| \leq C_2 |Q - P|^\alpha, \quad \hat{\mathbf{n}}_P := (\sqrt{1 + |\nabla f(P)|^2})^{-1} \mathbf{n}_P,$$

uniformly for all edges $\mathbf{e} = \mathbf{e}_{PQ}$. In other words, either $\hat{\mathbf{n}}_{\mathbf{e}}$ or $-\hat{\mathbf{n}}_{\mathbf{e}}$ should be very close to the unit normal $\hat{\mathbf{n}}_P$ to the surface Σ at the nearby point P . Obviously, P can be replaced by any other point at distance $\leq C|Q - P|$ from P on Σ . That this condition can be realized is guaranteed by the following

Proposition 2. *Under the conditions of Proposition 1, assume that $h(\mathbf{v}) \leq \bar{h}_1$. Then the unit normal to any of the two triangular faces attached to \mathbf{e} satisfies the above inequality with a constant C_2 depending on c, C_0, C_1 , only. More precisely, if $\mathbf{e} = \mathbf{v}_Q - \mathbf{v}_P$ and $\tilde{\mathbf{e}} = \mathbf{v}_{\tilde{Q}} - \mathbf{v}_P$ denote edges attached to P and belonging to one of these triangular faces then we have*

$$\min |\pm \mathbf{n}_{\mathbf{e} \times \tilde{\mathbf{e}}} - \hat{\mathbf{n}}_P| \leq 4C_1 C_0^\alpha c^{-(1+\alpha)} |Q - P|^\alpha.$$

Here, $\mathbf{n}_{\mathbf{u}} = |\mathbf{u}|^{-1} \mathbf{u}$ denotes the unit vector in direction $\mathbf{u} \neq \mathbf{0}$.



$$\hat{\mathbf{v}}_e = \frac{1}{2}(\mathbf{v}_Q + \mathbf{v}_P), \quad \hat{\mathbf{n}}_e = \mathbf{n}_{\mathbf{e} \times \mathbf{d}} = \mathbf{n}_{\mathbf{e} \times \tilde{\mathbf{e}} + \tilde{\mathbf{e}} \times \mathbf{e}}$$

Fig. 1. Notation used throughout the paper. Shown is the flap neighborhood of an edge $\mathbf{e} = \mathbf{v}_Q - \mathbf{v}_P$ in the spatial mesh, with the left triangle associated with the triangle $PQ\tilde{Q}$ in \mathcal{T} , the base point $\hat{\mathbf{v}}_e$, the approximate normal $\hat{\mathbf{n}}_e$, and the newly inserted intersection point \mathbf{v}_e of the normal line with Σ (not shown is Σ itself).

Proof. The notation used throughout this proof and at later occasions is given in Fig. 1. Elementary computations show that

$$\begin{aligned} \mathbf{e} \times \tilde{\mathbf{e}} &= (Q - P, f(Q) - f(P)) \times (\tilde{Q} - P, f(\tilde{Q}) - f(P)) \\ &= (Q - P, \nabla f(P)(Q - P) + \epsilon) \times (\tilde{Q} - P, \nabla f(P)(\tilde{Q} - P) + \tilde{\epsilon}) \\ &= 2A_{PQ\tilde{Q}}(-\nabla f(P), 1) + \mathbf{r} = 2A_{PQ\tilde{Q}}\mathbf{n}_P + \mathbf{r}, \end{aligned}$$

where $A_{PQ\tilde{Q}} = \pm \frac{1}{2} |(Q - P, 0) \times (\tilde{Q} - P, 0)|$ is the signed area of the triangle $PQ\tilde{Q}$ in \mathbb{R}^2 , and the remainder term \mathbf{r} can be estimated as

$$|\mathbf{r}|^2 \leq 2(\epsilon^2 |\tilde{Q} - P|^2 + \tilde{\epsilon}^2 |Q - P|^2)$$

$$\begin{aligned}
 &\leq 2C_1^2 |\tilde{Q} - P|^2 |Q - P|^2 (|\tilde{Q} - P|^{2\alpha} + |Q - P|^{2\alpha}) \\
 &\leq 2C_1^2 |\mathbf{e}|^2 |\tilde{\mathbf{e}}|^2 (|\mathbf{e}|^{2\alpha} + |\tilde{\mathbf{e}}|^{2\alpha}) \\
 &\leq 4C_1^2 |\mathbf{e}|^2 |\tilde{\mathbf{e}}|^2 \max(|\mathbf{e}|^{2\alpha}, |\tilde{\mathbf{e}}|^{2\alpha}).
 \end{aligned}$$

Since by (1) and part a) of Proposition 1

$$\max(|\mathbf{e}|, |\tilde{\mathbf{e}}|) \leq C_0 \max(|Q - P|, |\tilde{Q} - P|) \leq C_0 c^{-1} |Q - P|,$$

we arrive at

$$|\mathbf{r}| \leq 2C_1 |\mathbf{e}| |\tilde{\mathbf{e}}| (\max(|\mathbf{e}|, |\tilde{\mathbf{e}}|))^\alpha \leq 2C_1 C_0^\alpha c^{-\alpha} |\mathbf{e}| |\tilde{\mathbf{e}}| |Q - P|^\alpha. \quad (2)$$

Note that this inequality yields part b) of Proposition 1 with some $\bar{c} \geq c/(2C_0)$ since for small enough $h(\mathbf{v})$

$$\begin{aligned}
 \sin(\angle QP\tilde{Q}) &= \frac{|2A_{PQ\tilde{Q}}|}{|Q - P| |\tilde{Q} - P|} \geq \frac{|\mathbf{e} \times \tilde{\mathbf{e}}| - |\mathbf{r}|}{|\mathbf{n}_P| |Q - P| |\tilde{Q} - P|} \\
 &\geq \frac{|\mathbf{e}| |\tilde{\mathbf{e}}| (c - 2C_1 h(\mathbf{v})^\alpha)}{C_0 |Q - P| |\tilde{Q} - P|} \geq \frac{c}{2C_0}.
 \end{aligned}$$

The argument for the opposite direction of the statement in Proposition 1 b) is analogous, it will not be needed in this paper.

We apply next the elementary fact that

$$|\mathbf{n}_\mathbf{u} - \mathbf{n}_{\tilde{\mathbf{u}}}| \leq \frac{|\mathbf{u} - \tilde{\mathbf{u}}|}{\min(|\mathbf{u}|, |\tilde{\mathbf{u}}|)}$$

holds for any two non-zero directions $\mathbf{u}, \tilde{\mathbf{u}}$ to the following two particular vectors:

$$\mathbf{u} := \frac{\mathbf{e} \times \tilde{\mathbf{e}}}{2A_{PQ\tilde{Q}}}, \quad \tilde{\mathbf{u}} := \mathbf{n}_P = (-\nabla f(P), 1).$$

Since and $2A_{PQ\tilde{Q}}(\mathbf{u} - \tilde{\mathbf{u}}) = \mathbf{r}$, $2A_{PQ\tilde{Q}}\mathbf{n}_P = \mathbf{e} \times \tilde{\mathbf{e}} - \mathbf{r}$, and $\min(|\mathbf{u}|, |\tilde{\mathbf{u}}|) = \min(|\mathbf{n}_P|, |\mathbf{e} \times \tilde{\mathbf{e}}|/|2A_{PQ\tilde{Q}}|)$ by the notation introduced above, with the assumption $|\mathbf{e} \times \tilde{\mathbf{e}}| \geq c|\mathbf{e}| |\tilde{\mathbf{e}}|$ and (2) this yields

$$\begin{aligned}
 \min |\pm \mathbf{n}_{\mathbf{e} \times \tilde{\mathbf{e}}} - \hat{\mathbf{n}}_P| &\leq |\mathbf{n}_\mathbf{u} - \mathbf{n}_{\tilde{\mathbf{u}}}| \leq \frac{|\mathbf{r}|}{\min(|2A_{PQ\tilde{Q}}\mathbf{n}_P|, |\mathbf{e} \times \tilde{\mathbf{e}}|)} \\
 &\leq \frac{|\mathbf{r}|}{|\mathbf{e} \times \tilde{\mathbf{e}}| - |\mathbf{r}|} \leq \frac{2C_1 C_0^\alpha c^{-\alpha} |\mathbf{e}| |\tilde{\mathbf{e}}| |Q - P|^\alpha}{|\mathbf{e}| |\tilde{\mathbf{e}}| (c - 2C_1 h(\mathbf{v})^\alpha)}.
 \end{aligned}$$

Thus, for small enough $h(\mathbf{v})$, we arrive at the statement of Proposition 2.

Note that the slightly more symmetric with respect to \mathbf{e} choice of an approximate normal $\hat{\mathbf{n}}_\mathbf{e} := \mathbf{n}_{\mathbf{e} \times \mathbf{d}}$, where $\mathbf{d} := \mathbf{v}_{\tilde{Q}} - \mathbf{v}_{\tilde{Q}}$ is the other diagonal of the quadrilateral composed of the two triangular faces attached to \mathbf{e} , will satisfy the same distance bound

$$\min |\pm \mathbf{n}_{\mathbf{e} \times \mathbf{d}} - \hat{\mathbf{n}}_P| \leq C_2 |Q - P|^\alpha, \quad C_2 = 4C_1 C_0^\alpha c^{-(1+\alpha)}. \quad (3)$$

Indeed, since Proposition 2 applied to $\tilde{\mathbf{e}} \times \mathbf{e}$ with $\tilde{\mathbf{e}} = \mathbf{v}_{\tilde{Q}} - \mathbf{v}_P$ leads to the same estimate (and to the same sign for the area $A_{P\tilde{Q}Q}$), the linear combination

$$\mathbf{e} \times \tilde{\mathbf{e}} + \tilde{\mathbf{e}} \times \mathbf{e} = \mathbf{e} \times (\tilde{\mathbf{e}} - \tilde{\mathbf{e}}) = \mathbf{e} \times \mathbf{d}$$

must give it, too.

2.3 Normal MT with edge midpoint prediction

For better reference, and to introduce some auxiliary notation, we first investigate a single step of the normal MT considered in this paper. Let \mathcal{T} and \mathbf{v} be given. For each edge $\mathbf{e} = \mathbf{v}_Q - \mathbf{v}_P$, we compute base point and approximate normal:

$$\hat{\mathbf{v}}_{\mathbf{e}} := \frac{1}{2}(\mathbf{v}_Q + \mathbf{v}_P), \quad \hat{\mathbf{n}}_{\mathbf{e}} := \mathbf{n}_{\mathbf{e} \times \mathbf{d}}. \quad (4)$$

Then we find $\mathbf{v}_e \in \Sigma$ by intersecting the line $\hat{\mathbf{v}}_{\mathbf{e}} + s\hat{\mathbf{n}}_{\mathbf{e}}$ with Σ , and denote the corresponding parameter s by $d_{\mathbf{e}}$ (most of this notation was already introduced in Fig. 1). This way, we obtain a new triangular mesh with vertex set $\tilde{\mathbf{v}}$ composed of \mathbf{v} and the newly created points \mathbf{v}_e , its underlying triangulation $\tilde{\mathcal{T}}$ in \mathbb{R}^2 , and the detail vector $\tilde{\mathbf{d}}$ composed of the individual $d_{\mathbf{e}}$.

The following proposition states that for c -regular triangular meshes with small enough $h(\mathbf{v})$, the intersection step is safely executable, leads to a new triangular mesh with only slightly smaller regularity constant, and also delivers the bound $|d_{\mathbf{e}}| = O(|\mathbf{e}|^{1+\alpha})$. It is central for carrying out the recursion argument for proving our main result on normal MT in the next section.

Proposition 3. *Under the conditions of Proposition 1, there are positive constants $\bar{h}_2 \leq \bar{h}_1$ and C_3, C_4, C_5 , depending on the constants c, C_0, C_1, α , such that for any edge \mathbf{e} in a triangular mesh with $h(\mathbf{v}) \leq \bar{h}_2$, there exists a unique intersection point \mathbf{v}_e of the line segment $\{\hat{\mathbf{v}}_{\mathbf{e}} + s\hat{\mathbf{n}}_{\mathbf{e}} : |s| \leq |Q - P|/|\mathbf{n}_P|\}$ with Σ . The resulting detail coefficient $d_{\mathbf{e}}$ satisfies the estimate*

$$|d_{\mathbf{e}}| = |\mathbf{v}_e - \hat{\mathbf{v}}_{\mathbf{e}}| \leq C_3|Q - P|^{1+\alpha}.$$

The new triangular mesh given by $\tilde{\mathcal{T}}$ and $\tilde{\mathbf{v}}$ is \tilde{c} -regular with a constant

$$\tilde{c} \geq c(1 - C_4h(\mathbf{v})^\alpha),$$

and has mesh-width

$$h(\tilde{\mathbf{v}}) \leq \frac{1}{2}(1 + C_5h(\mathbf{v})^\alpha)h(\mathbf{v}).$$

Proof. Since

$$\frac{1}{2}(f(P) + f(Q)) = f(P) + \frac{1}{2}\nabla f(P)(Q - P) + \epsilon, \quad |\epsilon| \leq \frac{1}{2}C_1|Q - P|^{1+\alpha},$$

and by the definition of $\hat{\mathbf{n}}_{\mathbf{e}}$ and the calculations leading to Proposition 2

$$(1 + |\nabla f(P)|^2)^{1/2}\hat{\mathbf{n}}_{\mathbf{e}} = (-\nabla f(P), 1) + (D, \delta), \quad \sqrt{|D|^2 + \delta^2} \leq C_0C_2|Q - P|^\alpha,$$

we obtain the following parametrization

$$\mathbf{v}(t) = (P + (Q - P)/2 + t(-\nabla f(P) + D), f(P) + \nabla f(P)(Q - P)/2 + \epsilon + t(1 + \delta))$$

with parameter $t := s|\mathbf{n}_P| \in [-|Q - P|, |Q - P|]$ of the line segment under consideration. The condition $\mathbf{v}(t) \in \Sigma$ is thus equivalent to

$$\begin{aligned} & f(P) + \nabla f(P)(Q - P)/2 + \epsilon + t(1 + \delta) \\ &= f(P + (Q - P)/2 + t(-\nabla f(P) + D)) \\ &= f(P) + \nabla f(P)((Q - P)/2 + t(-\nabla f(P) + D)) + \tilde{\epsilon}(t), \end{aligned}$$

where

$$|\tilde{\epsilon}(t)| \leq C_1|(Q - P)/2 + t(-\nabla f(P) + D)|^{1+\alpha}.$$

After cancelation of equal terms on both sides, we obtain a scalar fix point equation

$$t = \phi(t) := \frac{\tilde{\epsilon}(t) - \epsilon}{1 + |\nabla f(P)|^2 + \delta - \nabla f(P)D}.$$

It is easy to verify that for small enough $h(\mathbf{v})$

$$\frac{d}{dt}(t - \phi(t)) \geq 0, \quad |\phi(t)| < |Q - P|, \quad t \in [-|Q - P|, |Q - P|].$$

For the first inequality, observe that in the interval of interest and small enough $h(\mathbf{v})$

$$\phi'(t) = \frac{\tilde{\epsilon}'(t)}{1 + |\nabla f(P)|^2 + \delta - \nabla f(P)D} = \frac{O(|Q - P|^\alpha)}{1 + |\nabla f(P)|^2 + O(|Q - P|^\alpha)},$$

since the definition of the above introduced function $\tilde{\epsilon}(t)$ yields

$$\begin{aligned} \tilde{\epsilon}'(t) &= \nabla f(P + (Q - P)/2 + t(-\nabla f(P) + D)) - \nabla f(P)(-\nabla f(P) + D) \\ &= O(|Q - P|^\alpha) = O(h(\mathbf{v})^\alpha). \end{aligned}$$

Similarly, the second inequality follows from

$$|\tilde{\epsilon}(t)| \leq C_1(|(Q - P)|(\frac{1}{2} + |\nabla f(P)| + |D|))^{1+\alpha} \leq C_1(2C_0^2|Q - P|)^{1+\alpha}.$$

Thus, $\psi(t) = t - \phi(t)$ is a continuous, monotonously increasing function on $[-|Q - P|, |Q - P|]$, and takes opposite signs at the endpoints of this interval, which implies that $\phi(t) = t$ possesses a unique solution $t_e = d_e(1 + |\nabla f(P)|^2)^{1/2}$. By the already available bounds on $\tilde{\epsilon}(t)$ and ϵ we get

$$\begin{aligned} |d_e| = |\mathbf{v}_e - \hat{\mathbf{v}}_e| &\leq |t_e| = |\phi(t_e)| \leq \frac{|\tilde{\epsilon}(t_e)| + |\epsilon|}{1 + |\nabla f(P)|^2 - |\delta| - |\nabla f(P)D|} \\ &\leq \frac{C_1((2C_0^2)^{1+\alpha} + \frac{1}{2})|Q - P|^{1+\alpha}}{\frac{1}{2}(1 + |\nabla f(P)|^2)} \leq C_3|Q - P|^{1+\alpha}, \end{aligned} \quad (5)$$

with $C_3 := C_1(1 + 2(2C_0)^{1+\alpha})$, if we choose \bar{h}_2 small enough. Observe that C_3 only depends on C_0, C_1, α , while \bar{h}_2 may also depend on c (e.g., via C_2).

The above estimate (5) for $|d_e| = |\mathbf{v}_e - \hat{\mathbf{v}}_e|$ the new triangular mesh $\tilde{\mathbf{v}}$ will be a small perturbation of the dyadic refinement $\hat{\mathbf{v}}$ obtained by edge midpoint insertion of the original triangular mesh \mathbf{v} . Any two adjacent edges $\mathbf{e}', \tilde{\mathbf{e}}'$ in the new mesh given by $\tilde{\mathbf{v}}$ are naturally associated with a triangle $PQ\tilde{Q}$ in \mathcal{T} , and with two edges $\mathbf{e}, \tilde{\mathbf{e}}$ of the triangular face in \mathbf{v} corresponding to it so that we can write

$$\mathbf{e}' = \pm \frac{1}{2}\mathbf{e} + \mathbf{r}, \quad \tilde{\mathbf{e}}' = \pm \frac{1}{2}\tilde{\mathbf{e}} + \tilde{\mathbf{r}}, \quad |\mathbf{r}|, |\tilde{\mathbf{r}}| \leq 2C_3\Delta^{1+\alpha}, \quad (6)$$

where $\Delta = \max(|Q - P|, |\tilde{Q} - P|, |Q - \tilde{Q}|)$. Indeed, each edge \mathbf{e}' is either connecting a newly inserted point \mathbf{v}_e with one of the endpoints of $\mathbf{e} = \mathbf{v}_Q - \mathbf{v}_P$ (say \mathbf{v}_P) in which case by (4)

$$\mathbf{e}' = \mathbf{v}_e - \hat{\mathbf{v}}_e + \frac{1}{2}(\mathbf{v}_P + \mathbf{v}_Q) - \mathbf{v}_P = \mathbf{r} + \frac{1}{2}\mathbf{e}$$

gives the result with $\mathbf{r} = \mathbf{v}_e - \hat{\mathbf{v}}_e$ estimated via (5), or it connects two new points \mathbf{v}_e and $\mathbf{v}_{\tilde{e}}$ corresponding to two adjacent edges $\mathbf{e} = \mathbf{v}_Q - \mathbf{v}_P$ and $\tilde{\mathbf{e}} = \mathbf{v}_{\tilde{Q}} - \mathbf{v}_P$ in \mathbf{v} associated with a triangle $\tilde{Q}PQ$ (note that this way any two adjacent edges $\mathbf{e}', \tilde{\mathbf{e}}'$ in $\tilde{\mathbf{v}}$ determine such a triangle uniquely). In the latter case, by using again (4) we can write

$$\mathbf{e}' = \mathbf{v}_{\tilde{e}} - \hat{\mathbf{v}}_{\tilde{e}} + \frac{1}{2}(\mathbf{v}_{\tilde{Q}} - \mathbf{v}_Q) + \hat{\mathbf{v}}_e - \mathbf{v}_e,$$

i.e., the third edge $\tilde{\mathbf{e}} = \mathbf{v}_{\tilde{Q}} - \mathbf{v}_Q$ corresponding to the triangle $\tilde{Q}PQ$ is now associated with \mathbf{e}' in (6), and (5) delivers the estimate for the remainder term $\mathbf{r} = (\mathbf{v}_{\tilde{e}} - \hat{\mathbf{v}}_{\tilde{e}}) + (\hat{\mathbf{v}}_e - \mathbf{v}_e)$.

Since for any triangle

$$\Delta \leq \max(|\mathbf{e}|, |\tilde{\mathbf{e}}|, |\tilde{\mathbf{e}}|) \leq \begin{cases} h(\mathbf{v}), \\ c^{-1} \min(|\mathbf{e}|, |\tilde{\mathbf{e}}|, |\tilde{\mathbf{e}}|), \end{cases}$$

the representation (6) gives

$$|\mathbf{e}'| \leq \frac{|\mathbf{e}|}{2} + |\mathbf{r}| \leq \frac{|\mathbf{e}|}{2} \left(1 + \frac{4C_3\Delta^{1+\alpha}}{|\mathbf{e}|}\right) \leq \frac{h(\mathbf{v})}{2} (1 + 4C_3c^{-1}h(\mathbf{v})^\alpha),$$

which implies the claimed bound for $h(\tilde{\mathbf{v}})$ with $C_5 := 4C_3c^{-1}$.

Similarly, for adjacent $\mathbf{e}', \tilde{\mathbf{e}}'$ by (6) one can write

$$\begin{aligned} \frac{|\mathbf{e}' \times \tilde{\mathbf{e}}'|}{|\mathbf{e}'||\tilde{\mathbf{e}}'|} &\geq \frac{|\mathbf{e} \times \tilde{\mathbf{e}}| - 2(|\mathbf{e}||\tilde{\mathbf{r}}| + |\tilde{\mathbf{e}}||\mathbf{r}| + 2|\tilde{\mathbf{r}}||\mathbf{r}|)}{|\mathbf{e}||\tilde{\mathbf{e}}| + 2(|\mathbf{e}||\tilde{\mathbf{r}}| + |\tilde{\mathbf{e}}||\mathbf{r}| + 2|\tilde{\mathbf{r}}||\mathbf{r}|)} \\ &\geq c \frac{1 - 2c^{-1}(|\mathbf{r}|/|\mathbf{e}| + |\tilde{\mathbf{r}}|/|\tilde{\mathbf{e}}| + 2(|\mathbf{r}||\tilde{\mathbf{r}}|)/(|\mathbf{e}||\tilde{\mathbf{e}}|))}{1 + 2(|\mathbf{r}|/|\mathbf{e}| + |\tilde{\mathbf{r}}|/|\tilde{\mathbf{e}}| + 2(|\mathbf{r}||\tilde{\mathbf{r}}|)/(|\mathbf{e}||\tilde{\mathbf{e}}|))}. \end{aligned}$$

Now substitute

$$\frac{|\mathbf{r}|}{|\mathbf{e}|} \leq 2C_3 \frac{|\Delta|^{1+\alpha}}{|\mathbf{e}|} \leq 2C_3 c^{-1} h(\mathbf{v})^\alpha,$$

and the similar estimate for $|\tilde{\mathbf{r}}|/|\tilde{\mathbf{e}}|$ to arrive at the bound for \tilde{c} . This concludes the proof of Proposition 3.

3 Main Result

We are now in a position to prove that the normal MT introduced in the previous section is well-posed for all $j \geq 1$, possesses the expected detail decay, and converges as $j \rightarrow \infty$, provided that the initial c -regular triangular mesh \mathbf{v}^0 mesh has small enough mesh-width (how small depends on the constants c, C_0, C_1 , and α). Convergence is understood as follows. Denote by $\tilde{\mathcal{T}}^j$ the triangulations in \mathbb{R}^2 obtained after j steps of uniform dyadic refinement from $\mathcal{T}^0 = \tilde{\mathcal{T}}^0$ (note that these triangulations are topologically equivalent and close to but generally different from the triangulations \mathcal{T}^j associated with \mathbf{v}^j if $j \geq 1$). Then we can define piecewise linear continuous vector functions $\mathbf{f}^j : \mathbb{R}^2 \rightarrow \mathbb{R}^3$ by piecewise linear interpolation of the values from \mathbf{v}^j at the vertices of $\tilde{\mathcal{T}}^j$. For the given class of Σ , we call the normal MT convergent for the initial mesh $\mathbf{v}^0 \subset \Sigma$ if \mathbf{f}^j converges uniformly to a continuous limit function $\mathbf{f} : \mathbb{R}^2 \rightarrow \mathbb{R}^3$ which we call normal re-parametrization of Σ .

Theorem 1. *Let Σ be a $C^{1,\alpha}$ graph surface with associated constants C_0, C_1 , and fix $c \in (0, \sqrt{3}/2]$. Then there exist constants C_6, C_7 , and $\bar{h} > 0$ depending on C_0, C_1, c, α only such that the normal MT described in Subsection 2.3 is well-posed for any c -regular \mathbf{v}^0 with $h(\mathbf{v}^0) \leq \bar{h}$ and all $j \geq 1$, converges to a $C^{0,1}$ re-parametrization \mathbf{f} of Σ , and satisfies*

$$\|d^j\|_\infty \leq C_6 2^{-(1+\alpha)j} h(\mathbf{v}^0)^{1+\alpha}, \quad h(\mathbf{v}^j) \leq C_7 2^{-j} h(\mathbf{v}^0), \quad j \geq 0.$$

Proof. Concerning the well-posedness of normal MT, we are almost there. The trick is to use the results from Section 2 with $\bar{c} < c$ (say $\bar{c} = c/2$), and apply Proposition 3 recursively. If c_j is the regularity constant after j successful steps of normal MT, and if $c_j \geq \bar{c}$, we can continue. Since lower bounds for c_j can be derived from Proposition 3, with a proper choice for \bar{h} we will be able to guarantee this for all $j \geq 1$. Here are the details. Let us tentatively assume that we have $c_j \geq \bar{c}$ for all $j \geq 0$, and set $h_j := h(\mathbf{v}^j)$. If $h_0 \leq \bar{h}_2$ for the constant \bar{h}_2 determined from $\bar{c}, C_0, C_1, \alpha$ in Proposition 3 then

$$h_1 \leq \frac{1}{2} h_0 (1 + C_5 h_0^\alpha) \leq \frac{1}{2} h_0 (1 + C_5 \bar{h}^\alpha),$$

and choosing $\bar{h} \leq \bar{h}_2$ such that also $C_5 \bar{h}^\alpha \leq \frac{1}{3}$ holds, we guarantee that $h_0 \leq \bar{h}$ yields $h_1 \leq \frac{2}{3} h_0 \leq \bar{h}$. By recursion, we thus get

$$h_j \leq \left(\frac{2}{3}\right)^j h_0, \quad j \geq 1.$$

Substituting this auxiliary result into the estimates in Proposition 3, we obtain

$$h_j \leq 2^{-j} h_0 \prod_{l=0}^{j-1} (1 + C_5 (\frac{2}{3})^{l\alpha} h_0^\alpha) \leq (1 + C h_0^\alpha) 2^{-j} h_0,$$

as well as

$$c_j \geq c \prod_{l=0}^{j-1} (1 - C_4 (\frac{2}{3})^{l\alpha} h_0^\alpha) \geq c(1 - C' h_0^\alpha),$$

possibly after decreasing \bar{h} further. Again, the constants C, C' in these bounds depend on $C_0, C_1, \bar{c}, \alpha$ only. Altogether, we see that for $\bar{c} = c/2$ there is \bar{h} (possibly smaller than mandated by earlier restrictions, to also satisfy $C' \bar{h}^\alpha \leq 1/2$) such that the normal MT starting from a coarse mesh \mathbf{v}^0 with $h_0 \leq \bar{h}$ is well-posed for all $j \geq 1$, and satisfies the stated decay estimates for h_j and $\|d^j\|_\infty$.

To establish convergence to a $C^{0,1}$ limit \mathbf{f} , it remains to observe that because of the definition of \mathbf{f}^j as piecewise linear interpolant of \mathbf{v}^j over the dyadic refinement \tilde{T}^j we have

$$\|\mathbf{f}^j - \mathbf{f}^{j-1}\|_C = \sup_{\mathbf{e}} |\mathbf{v}_{\mathbf{e}} - \hat{\mathbf{v}}_{\mathbf{e}}| \leq C_3 h (\mathbf{v}^{j-1})^{1+\alpha} \leq C_3 (C_7 2^{-j} h_0)^{1+\alpha},$$

where the supremum is with respect to all edges $\mathbf{e} = \mathbf{v}_Q - \mathbf{v}_P$ associated with \mathbf{v}^{j-1} , and notation and estimates from the proof of Proposition 3 have been recycled. This gives uniform convergence of \mathbf{f}^j to \mathbf{f} , together with the estimate

$$\|\mathbf{f}^j - \mathbf{f}\|_C \leq C_8 (2^{-j} h_0)^{1+\alpha}, \quad j \geq 0.$$

That \mathbf{f} is in $C^{0,1}$ is automatic from the fact that \mathbf{f}^j interpolates the graph surface Σ given by a $C^{1,\alpha}$ function f , and that mesh regularity is already guaranteed. Obviously, better than $C^{0,1}$ regularity cannot be expected for the reparametrization \mathbf{f} . We leave the detailed argument to the reader.

4 Discussion and Extensions

The above result is only a first step in the investigation of normal MTs for surfaces and other situations beyond the case of curves in \mathbb{R}^2 . Even in the partial case considered here, some questions are left open. Do we have well-posedness and convergence also for C^1 surfaces? Is this normal MT stable (see [3, 9] for the curve case)? Some applications and experimental results [14] suggest a need in investigating normal MTs for piecewise smooth (rather than globally C^1) surfaces. Finally, it is desirable to clarify the connection to research on manifold subdivision and multi-scale transforms, which builds on proximity conditions [18, 5] that seem to be implicitly present in the investigation of normal MTs for smooth surfaces, too.

One of the drawbacks of normal MTs for surfaces is that due to the more complicated surface topology they may fail independently of the choice of the

subdivision operator S for coarse or distorted meshes. This is the main reason for the density and regularity assumptions on \mathbf{v}^0 in our Theorem 1. Modifications of normal MTs to address this problem have already been discussed in [12]. In this respect, the situation for curves is better: Normal MT with linear B-spline S corresponding to edge midpoint insertion [3] resp. with the quadratic B-spline S (also called Chaikin’s corner cutting subdivision) [10] converge globally, i.e., without any assumptions on \mathbf{v}^0 , and can be used in the initial stages of the normal MT recursion to improve mesh properties before switching to the S of choice, compare [3, 8]. Guaranteeing global convergence for normal MTs in the surface case remains an open problem.

To serve possible applications such as surface compression [12] or front tracking algorithms in 3D applications [17], it is desirable that normal MTs guarantee as fast as possible detail decay by choosing more general S . It is known from the curve case that one can expect decay estimates $\|d^j\|_\infty = O(2^{-jr})$ for normal MT and $C^{k,\alpha}$ manifolds Σ ($k \geq 1$, $\alpha \in (0, 1)$), if $r \leq \min(k + \alpha, s_\infty(S) + 1, P_e)$, where $k + \alpha$ is the smoothness exponent of the manifold, $s_\infty(S)$ the Hölder smoothness exponent of S , and P_e its order of exact polynomial reproduction, see [3, 10] (note that for some S , equality is not admissible in the above bound for r). Similar results are expected to hold for the surface case, at least away from the extraordinary vertices induced by the initial mesh. For the simple S corresponding to edge midpoint insertion considered in the previous sections, we have $s_\infty(S) = 1$, $P_e = 2$, and thus $r \leq 1 + \alpha$ which is reflected in Theorem 1. Thus, improvements can only be expected for $C^{k,\alpha}$ manifolds with $k \geq 2$ and subdivision operators S with $P_e \geq 3$ and $s_\infty(S) > 1$. Examples that satisfy these conditions are the Butterfly scheme but also some interpolating schemes for $\sqrt{3}$ subdivision [6, 13, 11]. Loop subdivision, which was, together with the Butterfly scheme, practically tested in [12], does not provide better detail decay since for it $P_e = 2$ ($P_e \geq 3$ implies the existence of negative coefficients in the averaging rules defining S). The theoretical study of normal MTs for $C^{k,\alpha}$ graph surfaces Σ , more general S with $P_e \geq 2$ and $s_\infty(S) > 1$, and mesh topologies without extraordinary vertices is the subject of a forthcoming paper.

Here we provide results of some preliminary numerical experiments on detail decay with normal MTs based on linear, Loop, and Butterfly subdivision operators. Our example is the unit sphere, with four points as the initial point set \mathbf{v}^0 located in such a way that the underlying tetrahedron is non-degenerate but non-uniform. Such an initial topology has four vertices of valence 3, and for any scheme some precaution is necessary to achieve at least C^1 smooth meshes (re-parameterizations) near these extraordinary vertices of low valence. In Fig. 2, we compare on the left the decay of the detail coefficients stored in $\{|d^1|, |d^2|, \dots, |d^9|\}$, sorted by decreasing absolute value, for three normal MTs, namely with S defined by linear subdivision as theoretically investigated in Sections 2 and 3, Loop subdivision, and Butterfly subdivision, respectively. For the last two which were already tested in connection with surface compression in [12], extraordinary vertex treatment was implemented using the modifications originally proposed by Loop [15] and Zorin, Schröder, and Sweldens [19]. Ap-

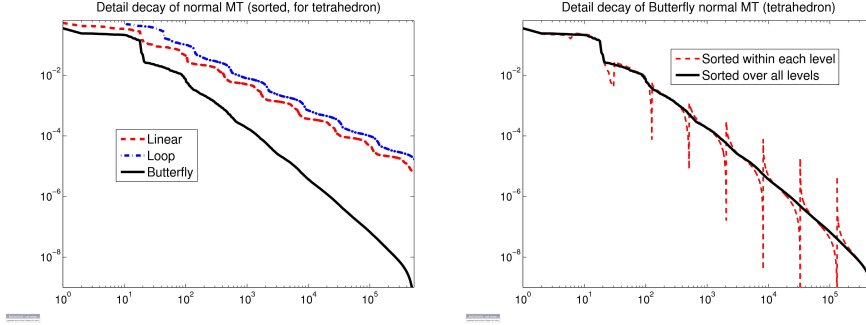


Fig. 2. Normal scheme for unit sphere with non-uniform tetrahedron at start. Left: Sorted detail plots for linear, Loop, and Butterfly normal MTs Right: Detail plot (sorted and unsorted) for the Butterfly normal MT.

proximate normals associated with base points corresponding to edge midpoints were computed by averaging the normals to the two attached triangular faces in the old mesh as described in Subsection 2.2 while for base point prediction close to vertices in \mathbf{v}^{j-1} as needed in Loop normal MT, a similar averaging of the normals to all triangular faces attached to this vertex was performed. Evidently, Butterfly normal MT produces much faster detail decay than linear and Loop normal MT. On the right of Fig. 2, for the Butterfly normal MT we show by the dashed line the same data $\{|d^1|, |d^2|, \dots, |d^9|\}$, but sorted only within each level. The slower decay of $\|d^j\|_\infty$ is due to the lower regularity of subdivision meshes at the four extraordinary vertices inherited from \mathbf{v}^0 . Larger $|d_i^j|$ values remain well-localized, and no pollution effect seems to occur (this is also documented by comparing with the solid line representing the detail sequence after sorting over all levels).

Level	Linear		Loop		Butterfly	
	$r_{j,\infty}$	$r_{j,2}$	$r_{j,\infty}$	$r_{j,2}$	$r_{j,\infty}$	$r_{j,2}$
2	0.5954	0.8378	0.9767	1.0404	0.5678	0.7648
3	1.9136	1.8983	1.4685	1.9634	3.0669	3.3070
4	1.8688	1.9448	1.8566	1.9735	2.4129	3.0355
5	1.9498	1.9834	1.9771	1.9857	2.1280	2.7896
6	1.9853	1.9955	2.0037	1.9959	2.0234	2.8613
7	1.9962	1.9988	1.9973	1.9990	2.0046	2.9190
8	1.9990	1.9997	1.9996	1.9997	2.0027	2.9569
9	1.9998	1.9999	1.9999	1.9999	2.0011	2.9772

Table 1. Approximate detail decay exponents for standard normal MTs

Table 1 provides more numerical evidence in support of these observations. We show approximations to the decay exponents r in the expected $O(2^{-jr})$ estimates for two norms of the detail sequences d^j , namely maximal and mean-square detail values

$$\|d^j\|_\infty = \max_{i=1,\dots,n_j} |d_i^j|, \quad \|d^j\|_2 = \left(n_j^{-1} \sum_{i=1}^{n_j} |d_i^j|^2 \right)^{1/2},$$

where n_j is the length of the sequence d^j . Note that n^j is smaller for interpolating than for approximating normal MTs, and is an argument in favor of using interpolating S in the construction of normal MTs. As indicator for the decay exponent characterizing the asymptotic decay of these norms, we used

$$r_{j,\alpha} := \log_2(\|d^{j-1}\|_\alpha / \|d^j\|_\alpha), \quad j = 2, \dots, 9, \quad \alpha = 2, \infty.$$

The values in Table 1 are in line with the predictions obtained by "extrapolating" results available from the theoretical analysis of normal MTs for curves in \mathbb{R}^2 to the surface case. In [3, 10], it has been shown that for normal MTs of smooth curves, the decay exponent r is restricted by two factors: the limit Hölder smoothness $s_\infty(S)$ of the linear subdivision scheme S , and its order of exact polynomial reproduction P_e . More precisely, $r < \min(P_e, s_\infty(S))$, with equality possible in certain cases. Similar results are expected to hold also for the surface case, at least, away from extraordinary vertices. Since $P_e = 2$, $s_\infty(S) = 1$ for linear subdivision and $P_e = 2$, $s_\infty(S) = 3$ for Loop subdivision (this is the H"older regularity exponent for regular triangulations, whereas the implemented modifications at extraordinary vertices guarantee $s_\infty(S) \geq 1$ in the general case), this explains the entries in the first four columns. Note that the first two columns show the sharpness of our Theorem 1 for $\alpha = 1$ since the sphere Σ is C^∞ , and thus $C^{1,1}$ smooth. For the Butterfly subdivision operator we have $P_e = 4$ and $s_\infty(S) = 2$ for regular mesh topologies (as far as we know, the latter statement has not yet been proved rigorously but only supported by numerical experiments), whereas $s_\infty(S) \geq 1$ holds in the general case. Thus, we expect a decay exponent close to $\max(P_e, s_\infty(S) + 1) = 3$ in the absence of extraordinary vertices, $r \geq 2$ in general. The numerical approximations $r_{j,\infty} \approx 2$ and $r_{j,2} \approx 3$ contained in the last two columns of Table 1 perfectly match these theoretical extrapolations, and also show that the presence of extraordinary vertices affects the decay rate of the maximal detail but can be neglected on average.

Finally, in Fig. 3 and Table 2, we compare the above standard MTs with the detail decay from a new combined scheme. The rationale of this scheme is based on the following observations: The normal Loop MT produces very smooth meshes but predicts base points far off the target surface, as it reproduces only linear polynomials exactly ($P_e = 2$). Normal Butterfly meshes are not as smooth but predicted base points are relatively close to the surface since this interpolating scheme reproduces cubic polynomials exactly on uniform meshes ($P_e = 4$). Both factors (limit Hölder smoothness $s_\infty(S)$ of the meshes and order of polynomial exactness P_e) are limiting the rate of detail decay. The idea of the

combined scheme is to use the normal Loop MT to find the meshes but instead of storing the relatively large details corresponding to the distance from the Loop-generated base point to the intersection point with the surface, another prediction with a scheme of high order of exact polynomial reproduction (in our case, the Butterfly scheme) should yield an improved base point along the same normal line, located at a distance asymptotically much smaller than either scheme alone could achieve. To be more precise, let S_B and S_L denote the linear Butterfly and Loop subdivision operators. Then, with \mathbf{v}^{j-1} at hand, the combined scheme computes \mathbf{v}^j as in the normal Loop MT by setting $\hat{\mathbf{v}}^j = S_L \mathbf{v}^{j-1}$, defining approximate normals $\hat{\mathbf{n}}^j$ as usual, and intersecting the resulting lines with Σ . What changes is the definition of details and the reconstruction formula. Denote $\tilde{\mathbf{v}}^j = S_B \mathbf{v}^{j-1}$, and define two sequences \tilde{d}^j, \hat{d}^j entry-wise by the formulas

$$\tilde{d}_i^j = (\mathbf{v}_i^j - \tilde{\mathbf{v}}_i^j) \hat{\mathbf{n}}_i^j, \quad \hat{d}_i^j = (\tilde{\mathbf{v}}_i^j - \hat{\mathbf{v}}_i^j) \hat{\mathbf{n}}_i^j.$$

Obviously, $d^j = \tilde{d}^j + \hat{d}^j$, and

$$\hat{\mathbf{v}}^j = \tilde{\mathbf{v}}^j + (\tilde{d}^j + \hat{d}^j) \hat{\mathbf{n}}^j.$$

What is stored as normal MT data for the combined scheme is now \tilde{d}^j , since everything else can be recovered from \mathbf{v}^{j-1} , at the expense of computing the additional vector $\tilde{\mathbf{v}}^j$.

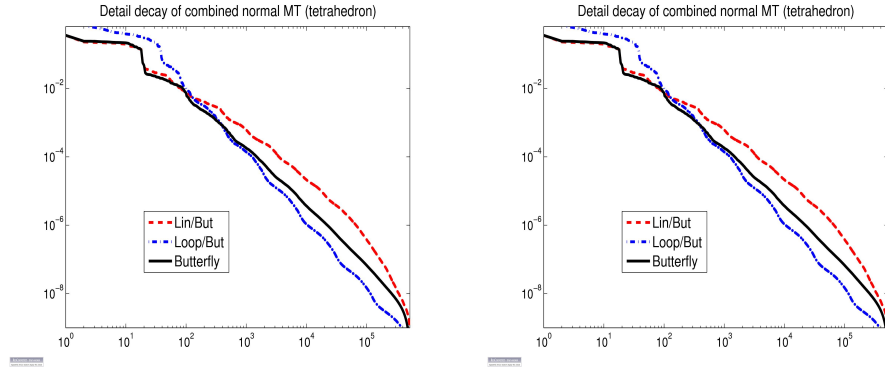


Fig. 3. Detail decay (sorted) for normal MTs (dashed line: combined Linear/Butterfly, solid line: Butterfly, dashed-dotted line: combined Loop/Butterfly schemes) for unit sphere with non-uniform tetrahedron (left) and double pyramid (right) as coarse mesh.

Each plot in Fig. 3 shows three curves, the sorted modified detail sequence $\{|\tilde{d}^1|, |\tilde{d}^2|, \dots, |\tilde{d}^9|\}$ for the new combined Loop/Butterfly normal MT, the similarly defined combined Linear/Butterfly normal MT, and (for comparison) the Butterfly normal MT which was the best one among the standard schemes. In addition to result with the non-uniform tetrahedron as \mathbf{v}^0 , we also show the test

results with a double-pyramid over a pentagon as \mathbf{v}^0 (this choice yields extraordinary vertices of valence 4 and 5). Note that although the detail sequences \tilde{d}^j to be stored for the new combined but non-interpolating Loop/Butterfly scheme are longer in comparison with the d^j stored for the interpolating Butterfly normal MT, the combined scheme is superior in the asymptotic range. The combination of linear normal MT with additional Butterfly-based base point prediction is not competitive due to the low limit smoothness of the associated meshes.

Level	Linear/Butt.		Loop/Butt.		Butterfly	
	$r_{j,\infty}$	$r_{j,2}$	$r_{j,\infty}$	$r_{j,2}$	$r_{j,\infty}$	$r_{j,2}$
2	0.7359	0.8993	0.5361	0.6114	0.5678	0.7648
3	2.5279	2.8563	2.6135	3.5637	3.0669	3.3070
4	2.0309	2.3733	3.2952	3.7820	2.4129	3.0355
5	2.1528	2.4372	3.8059	3.9327	2.1280	2.7896
6	2.0436	2.4801	3.9294	3.9824	2.0234	2.8613
7	2.0104	2.4926	3.9912	3.9953	2.0046	2.9190
8	2.0026	2.4969	3.9948	3.9986	2.0027	2.9569
9	2.0006	2.4986	3.9984	3.9995	2.0011	2.9772

Table 2. Approximate detail decay exponents for standard normal MTs

This is also documented by the corresponding approximations $r_{j,\alpha}$ of the decay exponents collected into Table 3 (again, the results for the standard Butterfly normal MT are included for better comparison). The observed approximations $r_{j,2}$ of decay exponents for the mean-square detail size on each level for the combined Loop/Butterfly scheme improve upon the stand-alone Loop and Butterfly normal MTs. That the asymptotic decay of maximal detail size $\|\tilde{d}^j\|_\infty$ expressed by $r_{j,\infty} \approx 4$ is as good the mean-square detail decay is somewhat surprising. For the combined Linear/Butterfly normal MT, the asymptotic behavior of these numbers is expectedly worse, and given by $r_{j,2} \approx 5/2$ and $r_{j,\infty} \approx 2$. We also performed tests with other initial \mathbf{v}^0 , e.g., the double pyramid, with almost identical outcome. The theoretical understanding of these empirical observations is still ahead.

References

1. Baraniuk, R., Janssen, M., Lavu, S.: Multiscale approximation of piecewise smooth two-dimensional functions using normal triangulated meshes. *Appl. Comput. Harm. Anal.* 19, 92–30 (2005)
2. Binev, P., Dahmen, W., DeVore, R.A., Dyn, N.: Adaptive approximation of curves. In: *Approximation Theory*, pp. 43–57. Acad. Publ. House, Sofia (2004)
3. Daubechies, I., Runborg, O., Sweldens, W., Normal multiresolution approximation of curves. *Constr. Approx.* 20, 399–462 (2005).

4. Friedel, I., Khodakovsky, A., Schröder, P.: Variational normal meshes. *ACM Trans. Graph.* 23, 1061–1073 (2004)
5. Grohs, P.: A general proximity analysis of nonlinear subdivision schemes. *SIAM J. Math. Anal.* 42, 729–750 (2010)
6. Guskov, I.: Irregular subdivision and its applications. PhD thesis, Princeton Univ., Dep. of Mathematics (1999)
7. Guskov, I., Vidimce, K., Sweldens, W., Schröder, P.: Normal meshes. In: *Computer Graphics Proceedings (Siggraph '00)*, pp. 95–102. ACM Press (2000)
8. Harizanov, S.: Globally convergent adaptive normal multi-scale transforms. *This Proceedings* (submitted)
9. Harizanov, S., Oswald, P.: Stability of nonlinear subdivision and multiscale transforms. *Constr. Approx.* 31, 359–393 (2010)
10. Harizanov, S., Oswald, P., Shingel, T.: Normal multi-scale transforms for curves. *Found. Comput. Math.* (submitted 2009, <http://www.faculty.jacobs-university.de/poswald>)
11. Jiang, J., Oswald, P.: Triangular $\sqrt{3}$ -subdivision schemes: the regular case. *J. Comput. Appl. Math.* 156, 47–75 (2003)
12. Khodakovsky, A., Guskov, I.: Compression of normal meshes. In: *Geometric Modeling for Scientific Visualization*, pp. 189–207. Springer, Berlin (2003)
13. Labsik, U., Greiner, G.: Interpolatory $\sqrt{3}$ -subdivision. *Computer Graphics Forum* 19, 131–139 (2000)
14. Lavu, S., Choi, H., Baraniuk, R.: Geometry compression of normal meshes using rate-distortion algorithms. In: *Eurographics/ACM Siggraph Symposium on Geometry Processing*, pp. 52–61. RWTH Aachen (2003)
15. Loop, C.: Smooth subdivision surfaces based on triangles. Master's thesis. Univ. of Utah, Dep. of Mathematics (1987)
16. Runborg, O.: Introduction to normal multiresolution analysis. In: *Multiscale Methods in Science and Engineering, LNCSE vol. 44*, pp. 205–224. Springer, Heidelberg (2005)
17. Runborg, O.: Fast interface tracking via a multiresolution representation of curves and surfaces. *Commun. Math. Sci.* 7, 365–389 (2009)
18. Wallner, J.: Smoothness analysis of subdivision schemes by proximity. *Constr. Approx.* 24, 289–318 (2006)
19. Zorin, D., Schröder, P., Sweldens, W.: Interpolating subdivision for meshes of arbitrary topology. In: *Computer Graphics Proceedings (SIGGRAPH '96)*, pp. 189–192, ACM Press (1996)